COMPARISON OF CONTROL STRATEGIES OF RESIDENTIAL PV STORAGE SYSTEMS

Matthias Resch[1], Bagus Ramadhani[2], Jochen Bühler[1], Andreas Sumper[3]

[1]Reiner Lemoine Institut gGmbH, Ostendstraße 25, 12459 Berlin, Germany
Phone +49 (0)30 5304 2013, E-mail: matthias.resch@rl-institut.de
[2]Postgraduate Programme Renewable Energy, University of Oldenburg, Carl-von-Ossietzky-Str. 9-11, 26129 Oldenburg
[3]UPC - Universitat Politècnica de Catalunya, 187 Carrer Comte d'Urgell, 08036 Barcelona, Spain

Abstract - The increase of renewable energy penetration in the distribution grid creates a problem concerning the power quality. One of the most critical scenarios occurs in times of excessive power generation combined with low load consumption, which may lead to an overvoltage due to reverse power flows. Grid expansion is often used as a solution to reduce the voltage rise. However as this new cables or transformers are only used a few hours per year, energy storage might be used as a voltage support among other alternatives. This research is embedded in the project SmartPower-Flow[1], which deals with the optimization of grid expansion versus energy storage at low voltage levels, where the grid expansion results due to increasing renewable power flows. Since both community and residential batteries have their own control and are connected to the same grid, the interaction between these battery systems has to be studied. This study focuses on residential batteries. Current control strategies for residential photovoltaic (PV) storage systems do not efficiently use the battery as a grid voltage support. Therefore, an investigation on the more intelligent control strategy has been conducted. The objective of the study is to determine the best control strategy for residential PV storage systems in Germany based on technical and economic perspectives. The strategy should be able to control the voltage at the point of common coupling (PCC) while still exhibiting a high self-consumption rate (SCR). Finally a qualitative evaluation of the strategies in respect of the SCR, the self-supply ratio (SSR), the curtailment losses rate (CLR) and the ability to limit the peak voltage at the point of common coupling (PVR) is presented.

I. INTRODUCTION

The decrease of feed-in tariffs in Germany is the main driver that makes the PV systems became less profitable. Together with increasing electricity prices maximizing the local consumption from the electricity produced by the PV is considered to be more beneficial than injecting the power into the grid. As the self-consumption rate might be increased by combining the battery with the PV systems, more and more residential PV owner consider investing in PV storage systems rather than in pure PV systems.

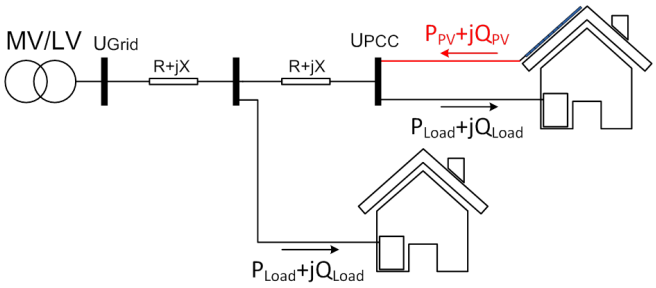

Figure 1: Bi-directional power flow in distribution grids

Figure 1 and figure 2 illustrate the influence of PV systems on the voltage at the PCC. Without PV generators, the voltage drop will occur on the feeder due to a power flow from the grid to the households. Once the PV system is connected to the grid, the voltage at the PCC is likely to be increased due to the reverse power flow back to the grid. The voltage rise at the PCC can be approximated by equation (I.1) [1],

[1]funded by the Federal Ministry of Economics and Technology (BMWi) under grant agreement no. 0325522A.

and it can be seen that the voltage rise is the function of the grid voltage (U_{grid}) and its conjugate (U^*_{grid}), the impedance of the grid (R+jX) and the active power P and reactive power Q of the PV system. Several solutions may be implemented in the low voltage distribution grid in order to solve the overvoltage problem and meet the voltage limit that is described in EN 50160, and which requires, that the 10-minute rms average of the voltage at the PCC is to remain within an interval of ±10 % of nominal voltage [2].

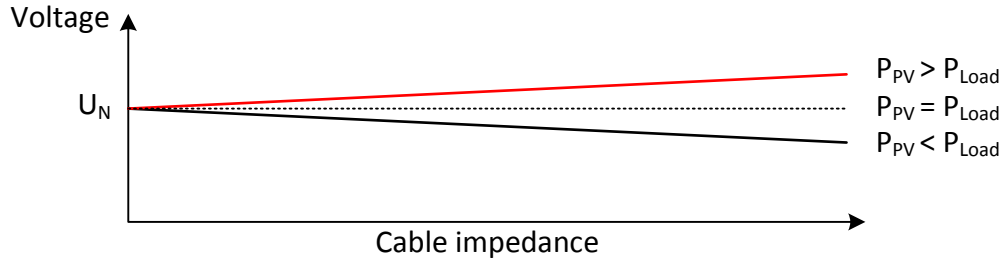

Figure 2: The impact of the power and the impedance on the grid

$$\Delta U = I \cdot (R + jX) = \frac{P - jQ}{U^*_{grid}} \cdot (R + jX) = \frac{PR + QX}{U^*_{grid}} + j\frac{PX - QR}{U^*_{grid}} \quad \text{(I.1)}$$

$$U_{PCC} = U_{grid} + \frac{PR + QX}{U^*_{grid}} + j\frac{PX - QR}{U^*_{grid}} \quad \text{(I.2)}$$

A solution might be obtained on the hardware level and/or the software level [3]. The following are some options that may be considered.

Hardware:

- Grid extension
- Automatic tap changer in local power transformers
- Energy storage

Software:

- Feed-in power limitation
  The voltage rise on the grid can be limited by limiting the feed-in power into the grid. The feed-in power can be controlled by reducing the output active power of the PV (controlled by the maximum power point tracking) or by using the power to charge the battery.
- Reactive power control
  According to equation (I.2), a reactive power control can be used to ensure voltage stability. The voltage at the PCC can be reduced by absorbing reactive power. However, due to the typically high R/X ratio of the low voltage distribution network, the required reactive power might also be high. In Germany, three different voltage regulation possibilities for distributed generators connected to the low voltage grid have been proposed [4]:
  - ***Fixed cosφ:*** A fixed amount of reactive power will be supplied/ absorbed by the distributed generators.
  - ***cosφ (P):*** In cosφ (P) control, the reactive power supply/ absorption is based on the active power output. The reactive power starts to be absorbed by the inverter when the active power reaches a certain threshold.
  - ***Q (U):*** Instead of following the active power, the reactive power absorption is based on the voltage at the PCC. The reactive power required will be calculated based on the droop characteristics provide by the DSO.

This study focusses on solving the overvoltage problem by using residential energy storages at the hardware level and feed-in power limitation and reactive power control on the software level.

In order to support the PV owner and to solve the overvoltage problem, the German government has introduced an incentive program for PV storage systems. The program will financially support the battery for a grid connected PV systems up to 30 kW_p. The elements of the program include a soft loan with an interest rate starting from 1.4 %. An additional rebate of 30 % of the costs of the battery will be granted once the project is successfully conducted and meets requirements. As the purpose of the program is mainly to prevent voltage violation caused by the residential PV systems, one of the requirement is to limit the feed-in power to 60 % [5]. Due to this limitation, an intelligent control strategy is required to ensure the compliance with the limit of feed-in power without losing residual energy. In this study four performance indicators are used to evaluate the control strategies:

- Self-consumption ratio (SCR)
  The SCR is given by

$$SCR = \frac{E_{PV_{consumed}}}{E_{PV}} \tag{I.3}$$

  where $E_{PV_{consumed}}$ is the consumed PV production and E_{PV} the PV production. As stated previously, an increase of the price of electricity and a decrease of the feed-in tariff creates the incentive to use PV energy production for the own consumption.

- Self-supply ratio (SSR)
  The SSR is given by

$$SSR = \frac{E_{PV_{consumed}}}{E_{load}} \tag{I.4}$$

  where $E_{PV_{consumed}}$ is the consumed PV production and E_{load} the load demand. A high self-supply ratio indicates that the PV-storage-systems can fulfill own load demand.

- Peak voltage reduction ratio (PVR)
  The control strategy should be able to control the voltage at the point of common coupling. It can be archieved by either using the storage to shave the peak or control active and reactive power. The PVR is defined as the ability of the control strategy to reduce the peak voltage, and is given by

$$PVR = \frac{U_{peak\ without\ control} - U_{peak\ with\ control}}{U_{peak\ without\ control} - U_n} \tag{I.5}$$

  where $U_{peak\ without\ control}$ is the highest voltage at the PCC without control strategy, $U_{peak\ with\ control}$ the maximum voltage at the PCC with control strategy and U_n the nominal voltage at the PCC.

- Share of losses ratio (LR)
  The share of losses of different control strategies are the combination of curtailment losses, losses due to reactive power compensation, inverter losses, and battery losses. The losses have to be minimized by using smart power management. The losses ratio is given by

$$LR = \frac{E_{losses}}{E_{PV}} \tag{I.6}$$

  where E_{losses} is the total loss and E_{PV} the PV production.

II. METHODOLOGY

In this chapter, the methodology of the investigation is described. The comparison of the control strategies of this paper is based on a literature study of different strategies proposed by several research groups and the application of those strategies through simulations. The six most promising strategies that show high self-consumption rate, ability to limit the voltage at the PCC and low losses have been further investigated and compared with a state-of-the-art strategy.

The simulations have been realized in two steps in order to examine the behaviour of each control strategy. The first step is the implementation of the algorithms of each control strategy in MATLAB and Excel. The outputs of the first step are the power flows for each strategy (power to charge the battery, power that is fed into the grid...). These results are then used in a second step by performing a load flow simulation in 1-min-steps with the commercial software PSS Sincal, which allows an evaluation of the ability of each strategy to control the voltage rise on different nodes for a test grid.

In the first step every control strategy is applied on two cases with different irradiance levels and load profiles. The battery size for this system is selected such as to achieve high degrees of self-consumption and self-supply rates. The optimal ratio according to [6] is 1 kWh of battery capacity per 1kWp PV system. A 5 kWp PV system and a 5 kWh battery have been chosen. To increase the lifetime of the battery, the operation range of the battery is limited from 20 % to 90 % state of charge (SOC). The PV power data is based on the measured data of a 121 kWp PV system in Allgäu (southern Germany) and normalized to 5kWp. Two dates with different irradiance level are used: 22-03-2013 (high irradiance) and 23-03-2013 (low irradiance). The load profiles are based on the standard load profile of a typical household (H0) in Germany with an annual consumption of 4.5 MWh/a [7]. The load profiles of a workday and a day at the weekend in autumn were used for the day with high and low irradiance respectively. The sampling rate of the original PV power data and the load profile are 15 minutes steps. The data was linearly interpolated to a 1-minute sampling rate to get a higher resolution data. Figure 3 shows the power flows without any control strategy in both cases.

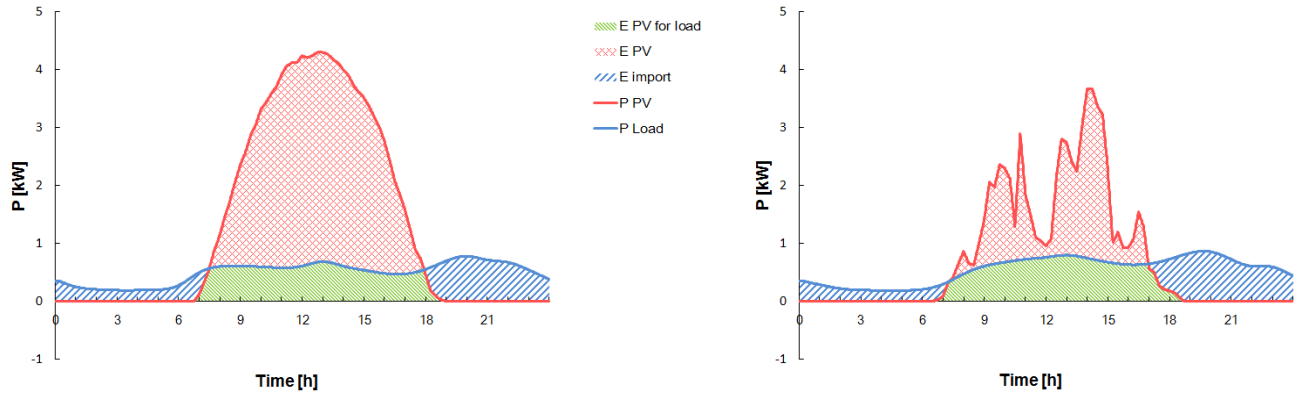

Figure 3: Power flows on high (left) and low irradiance day (right) without any control strategy

For the load flow calculation in step 2 a typical low voltage distribution grid in south Germany [8] with a high PV penetration of 20 x 5kWp PV-storage-systems has been used (figure 4). Detailed data of the grid is listed in table 1. The simulation has been performed using the load profile module of the software PSS Sincal. Pre-calculated 1-minute data from the first step of the simulation have been used as input data of the PVs, batteries, and loads in PSS Sincal. Finally, the voltage at the most critical node, the end of the string (PCC12), has been examined and the PVR has been calculated in order to compare the ability of the control strategies to reduce the voltage at PCC12. Additionally the other three performance indicator (SCR, SSR and LR) for each control strategy have been compered.

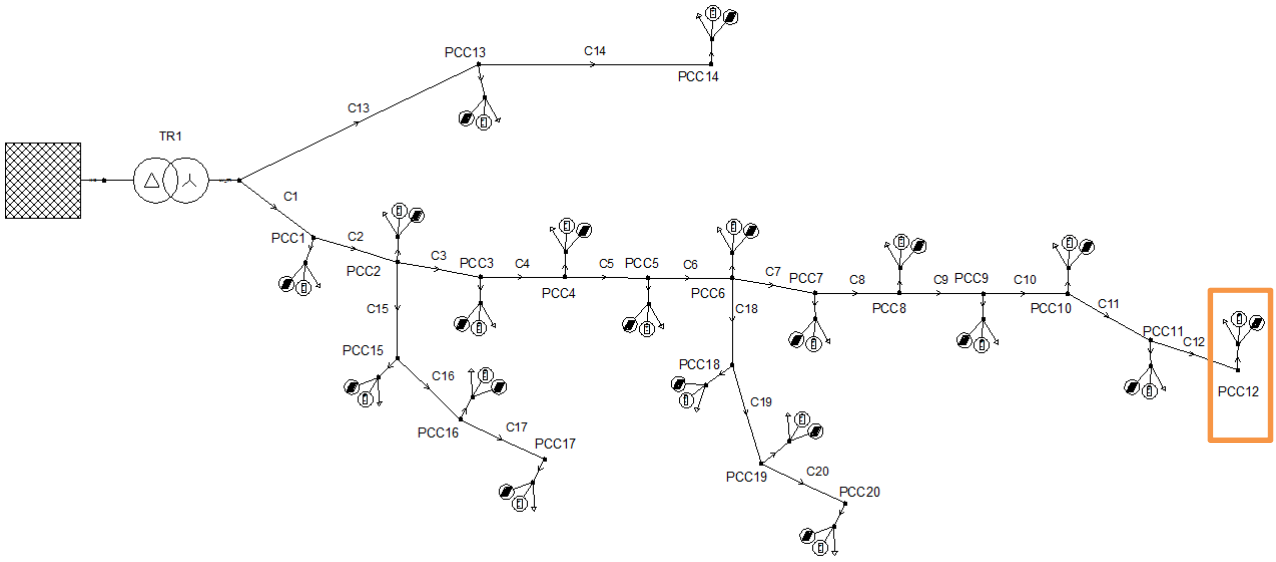

Figure 4: Typical LV distribution network with 20 x 5kWp PV-Storage-System

Table 1: LV distribution network specification

Utility grid	S_K''=100 MVA; R/X=0,1
Transformer	20/ 0.4 kV; S_n=160 kVA; Dyn5; U_k= 4 %
Feeder cable (C1-C12, C15-C20)	NAYY 4x 150 mm²; l=53 m; R=0.206 Ω/km; X=0.091 Ω/km
Feeder cable (C13-C14)	NAYY 4x 150 mm²; l=175 m; R=0.206 Ω/km; X=0.091 Ω/km
Cable from house to PCC	NAYY 4x 50 mm²; l=53 m; R=0.641 Ω/km; X=0.085 Ω/km
PV system	PV output profile
Battery	Charging power and discharging power profile
Load	Load profile

To simplify the simulation the following assumptions have been made:

- All PV-storage-systems use the same strategy and have the same PV power output and load profile.
- The efficiency of the battery and DC/DC converter has been neglected.
- The initial capacity of the battery is assumed to be 100 %.
- No weather and load forecast data have been considered. Strategies that require forecast data have been calculated with a perfect forecast.
- As for power losses, only curtailment losses have been taken into account.

III. RESULTS

In this chapter the control algorithm of seven control strategies and the corresponding power flows, their capability to charge the battery at the end of the day and voltage results are presented.

1. Self-consumption (state-of-the-art)

As mentioned previously, the storage of energy in the battery and the supply of energy for the own demand when there is no radiation might be beneficial for the system owner due to the difference in the feed-in tariff and the price of electricity consumption [6], [9]. The main objective of this control strategy is to improve the self-consumption rate and limit the voltage rise by limiting the feed-in power and reactive power compensation using cosφ (P) control. The simple algorithm makes this strategy likely to become the commonly used strategy for residential PV storage systems. In this strategy the battery is being fully charged as soon as possible by prioritizing the output power of the PV (P_{PV}) to supply the load and furthermore charge the battery (P_{Bat_ch}).

The algorithm and the power flows of the self-consumption strategy are depicted in figure 5. The figure shows the residual power of the PV system, the state of charge of the battery (SOC_{Bat}) and the voltage based on a load flow at PCC12. The SOC of the battery is calculated according to formula (III.2).

$$P_{Res} = P_{PV} - P_{Load} \tag{III.1}$$

$$SOC_{Bat} = 20\% + SOC_{Bat}(0) + SOC_{Bat} + \int \frac{P_{Bat}(t)}{Q_{Bat}} dt \tag{III.2}$$

The modes of operation are described in algorithm 1 (figure 5 (a)). In operation mode A, since P_{PV} is smaller than P_{Load} and the battery is fully discharged, power is imported from the grid in order to meet the demand. In mode B, the residual power P_{Res} charges the battery until reaching a SOC_{Bat} of 90 %. Once the battery is fully charged, the residual power is limited to 60 % of $P_{PV,\ mpp}$ to get incentives and is injected into the grid ($P_{Feed\text{-}in}$) (see mode C). In this period, the voltage is increased due to the reverse power from the PV into the grid. The voltage rise might be reduced by inductive reactive power compensation offered by the inverter. Therefore, the inverter is equipped with cosφ (P) control in order to regulate the amount of reactive power

$$Q_{PV} = \frac{P_{PV} - 0.5 \cdot P_{PV,mpp}}{0.5 \cdot P_{PV,mpp}} \cdot \tan(\arccos(0.95)) \tag{III.3}$$

that has to be absorbed, where $P_{PV,mpp}$ is the nominal output power of the PV system. In mode D, P_{PV} is smaller than P_{load} and the battery is not empty, therefore the battery is discharged to supply the load.

Concluding the self-consumption rate and self-supply rate are increased by implementing this strategy. As it can be seen in figure 5, using this strategy, the battery can get fully charged before noon and the power used later on to supply the load. However, the drawback of this strategy is that an excessive load on the grid might occur during the peak irradiation if there is no limitation on the PV output and therefore increase of the voltage at the PCC. On the other hand, if $P_{Feed\text{-}in}$ is limited to 60 %, there is a significant amount of curtailment losses on the day with high irradiance. Furthermore, limiting the feed-in power to 60 % does not guarantee that the voltage will remain below the critical limit on the grid with high PV penetration [1], [10].

Implementing a cosφ(P) control has also drawbacks for the grid. Since the reactive power absorbed is based on the active power, there might be unnecessary reactive power absorbed by the inverter even if the voltage is within the acceptable range. Besides, the system does not take into account the location of the PV system installed. All the PV systems in the feeder would be requested to absorb the same amount of reactive power [11].

(a)

Algorithm 1: Self consumption

Input: SOC_{Bat} = 20% to 90%, P_{PVp}, P_{PV}, P_{load}

for *t=00:00 to 23:59 step 00.01* **do**

- **if** $P_{PV}(t) > P_{Load}(t)$ *and* $SOC_{Bat}(t) < 90\%$ **then** /* Mode B */
  - $P_{Bat\_ch}(t) \leftarrow P_{Res}(t)$;
- **else if** $SOC_{Bat} = 90\%$ *and* $0 < P_{Res}(t) \leq 60\%\ P_{PVp}$ **then** /* Mode C */
  - $P_{Feed\text{-}in}(t) \leftarrow P_{Res}(t)$;
- **else if** $P_{Res} > 60\%\ P_{PVp}$ **then** /* Mode C */
  - $P_{Feed\text{-}in}(t) \leftarrow 60\%\ P_{PV}(t)$;
- **else if** $P_{PV}(t) < P_{Load}(t)$ *and* $SOC_{Bat}(t) > 20\%$ **then** /* Mode D */
  - $P_{Load}(t) \leftarrow P_{Bat\_dis}(t)$;
- **else** $P_{Load}(t) \leftarrow P_{Import}(t)$; /* Mode A */
- **if** $P_{PV}(t) > 50\%\ P_{PV}(t)$ **then** /* Reactive power compensation ($\cos\varphi(P)$) */
  - $Q_{PV}(t) \leftarrow Q_{PV}(t, P_{PV})$;
- **else** $Q_{PV}(t) \leftarrow 0$;

end

(b)

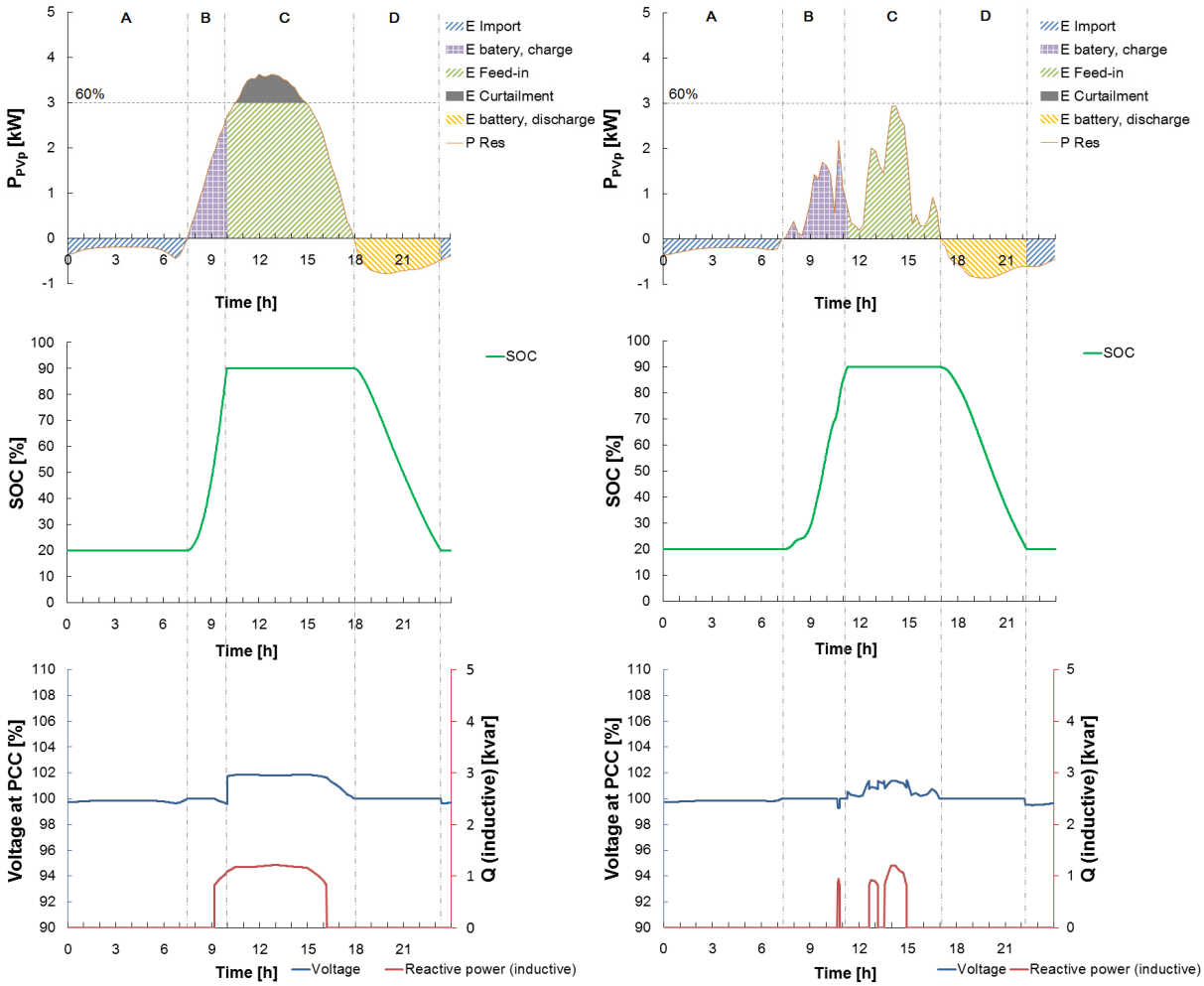

(c)

(d)

Figure 5: (a) algorithm, (b) power flows, (c) SOC and (d) voltage and reactive power at the PCC 12 of the self-consumption strategy on a high (left) and a low (right) irradiance day

2. Schedule mode

An alternative strategy to reduce the power losses and mitigate the voltage rise has been proposed by Struth et al. [9] and Ueda et al. [12]. In this strategy, the time to charge the battery will be shifted to a typical time with high radiation. The mode for charging the battery is activated from 11.30 until the battery is fully charged [9]. The principle operation of this strategy is shown in figure 6. The algorithms of mode A and D are similar to the previous strategy. In mode B however, when $P_{PV} > P_{Load}$ the residual load is limited to 60 % P_{PVmpp} and is injected into the grid until the activation of the charging mode is triggered, instead of directly charging the battery.

At 11:30, the residual power is used to charge the battery until the battery is fully charged (mode C). The limited residual load is injected into the grid again until P_{Res} is zero. In order to support the voltage at the PCC, reactive power compensation is also introduced in this strategy. Instead of the cosφ(P) control, a reactive power control Q(U) is used. The inverter starts to absorb the reactive power once the voltage at PCC reaches the threshold U_{start}. The amount of reactive power absorbed will be based on the droop characteristics from the distribution system operator (DSO) [13]. In this simulation, U_{start} is set to 1.005 p.u., and the reactive power absorption will be increased steadily until the voltage reaches 1.045 p.u.. At 1.045 p.u., the reactive power will be absorbed at a maximum value of cosφ=0.95. The amount of reactive power absorbed is calculated by:

$$Q_{PV} = \frac{U_{PCC} - U_{start}}{U_{start}} \cdot 25.125 \cdot \tan(\arccos(0.95)) \tag{III.4}$$

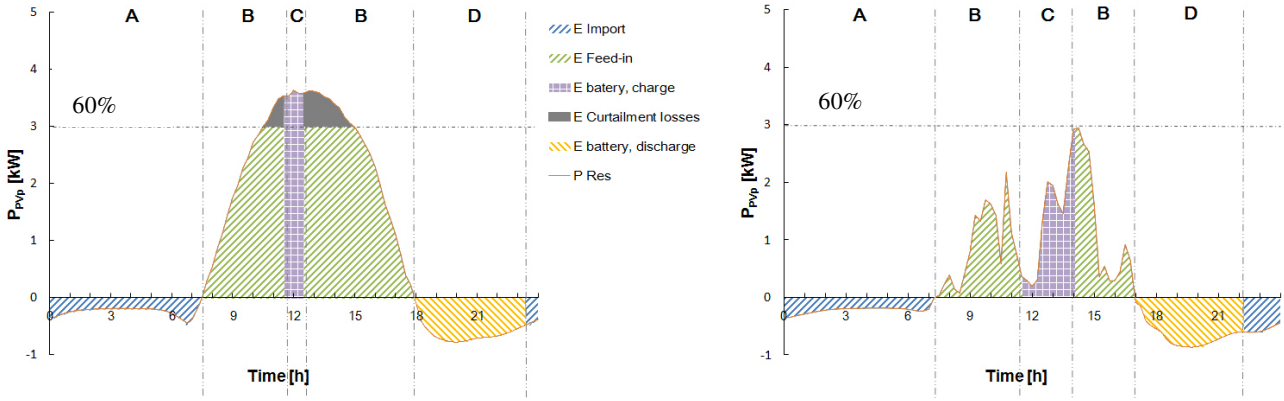

Figure 6: Power flows of the schedule mode according to [9] on a high (left) and a low (right) irradiance day

3. Schedule mode with constant charging power

Williams et al. [14] proposes a similar control strategy with time activation [14]. The difference to the previous strategy is that the battery is charged from 09:00 to 15:00 with constant charging power. This is done in order to avoid the battery from being fully charged before the end of the schedule. The charging power is defined as:

$$P_{Bat\_ch} = \frac{Q_{Bat}}{t_{start\_charge} - t_{stop\_charge}} \tag{III.5}$$

Where Q_{Bat} is the capacity of the battery, t_{start_charge} is the time where the charging process of battery is started and t_{stop_charge} the time when it is stopped.

Mode B operates as in the strategy “schedule mode”, except from 09:00 to 15:00 (mode C), where the battery is charged with the calculated power, and the remaining power is injected into the grid with the maximum of 60 % of P_{PVmpp}.

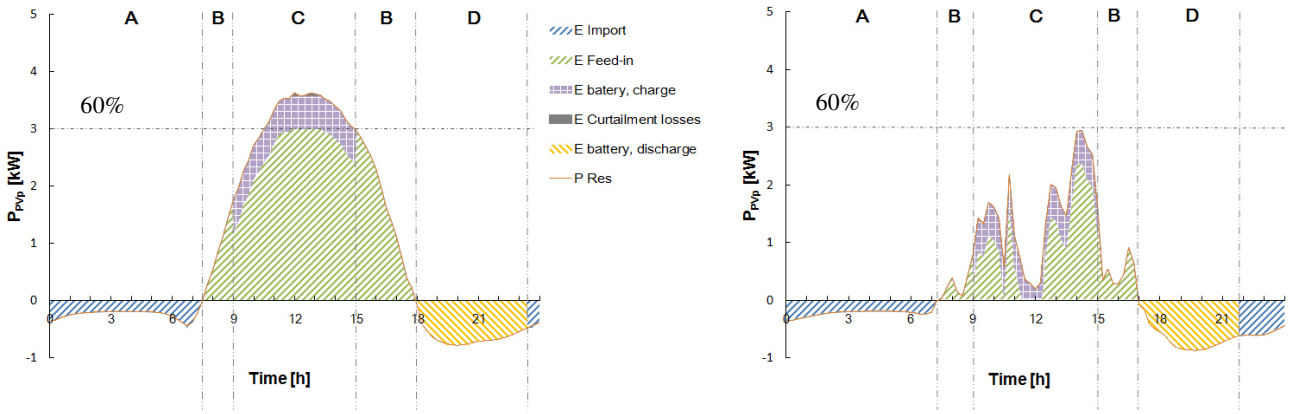

Figure 7: Power flows of the schedule mode according to [14] on a high (left) and a low (right) irradiance day

As shown in figure 6 and figure 7, both strategies use a time-shifting approach to mitigate the voltage rise. However, the second strategy with a time interval and limited charging rate is more promising compared to the one using the entire residual power to charge the battery. This can be seen from the lower curtailment losses of the strategy with constant charging power. The main drawback of this strategy is that the self-consumption rate might be slightly reduced if there is not enough radiation during the charging period. Reactive power compensation with Q(U) control is applied to both strategies. Furthermore, a drawback of using Q(U) control is the limitation of the inverter size. A significant amount of reactive power might be required to reduce the voltage at PCC which might be caused either by own PV power production or external PV. Moreover, the PV storage systems that are located at the end of the feeder might work at a higher power than the one close to the transformer due to the cable impedances. To solve this problem, an impedance-dependent parameterization of the Q(U) curve has been analyzed by Kerber [8]. This proposal is not implemented in any regulation yet.

4. Fixed feed-in limit

The objective of a fixed feed-in limit strategy is mainly to avoid the voltage rise by limiting the feed-in power and use the remaining residual power to charge the battery [1], [6], [10]. The limitation of the feed-in should be based on the voltage at the PCC, the power range of the battery, and the PV penetration on the grid [1]. In this case $P_{Feed\text{-}in}$ is set to 50 % although there is no guarantee that the voltage will be below the critical limit at high PV penetration. To reduce the voltage rise, reactive power compensation is also equipped in this strategy. Von Appen et al. [10] propose the combination of a fixed feed-in power, battery charging strategy, Q(U) control, and power curtailment in a multi-level voltage support. This strategy is the one examined in this study.

The simulated power flows of this operation strategy are shown in figure 8. The modes of operation A and E are similar to the import of power from the grid and the discharging battery algorithms of the previous strategies. In mode B, the residual power is injected into the grid until the residual power reaches 50 %. The feed-in power is fixed to 50 % and the remaining residual power is used to charge the battery, as shown in mode C. The Q(U) control is activated when the voltage reaches the threshold. However, since the power factor is limited by the inverter, the reactive power might reach the maximum while the voltage is still above the limit. In order to further reduce the voltage, the entire residual power is used to charge the battery. If the voltage is still above the limit and battery is fully charged, then the PV output power is curtailed. In mode D, if the residual power is less than 50 % and the battery is still not fully charged, the entire residual power is used to charge the battery (see figure 8 right). This last opportunity to charge the battery is helpful to increase the self-consumption rate especially on days with low irradiance. However the last opportunity to charge the battery will only be activated once the residual power reaches 50 %. This might lead to the possibility that the battery is not being charged during the day.

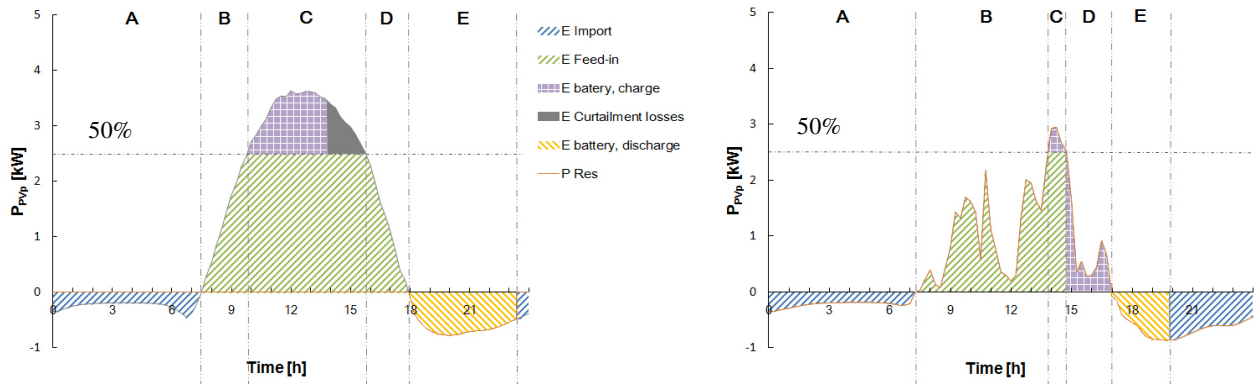

Figure 8: Power flows of the fixed feed-in strategy according to [10] on a high (left) and a low (right) irradiance day

The advantage of this strategy is that the voltage might be suppressed by limiting the feed-in power and absorbing reactive power. The problem is raised during cloudy or foggy days, when there is not enough radiation to charge the battery. Consequently, the self-consumption rate will be reduced. On the other hand, during high irradiance days, the power curtailment is high as can be seen in figure 8 (left). To avoid these losses, an optimization of the feed-in limit is proposed in the next strategy.

5. Dynamic feed-in limit

As a fixed feed-in limit leads to power curtailment during high irradiance days and reduces the self-consumption rate during low irradiance days, the dynamic feed-in limit strategy is introduced in this chapter. In order to overcome the problems, several strategies use weather and load predictions to dynamically adjust the feed-in limit, as described in [6], [9], [14], [15], [16].

The main goal of the strategy is to get a fully charged battery at the end of the day by adjusting the charging power and feed-in power. Load and weather forecast data of are used to get the optimized charging power during the day $P_{Bat\_ch\_pred}$ (equation (III.6)). The global horizontal irradiance data and ambient temperature is used to calculate the PV power output P_{PV_pred} based its location, orientation, and specification. The SOC of the battery is estimated for the entire day in order to be used as a predicted SOC. The feed-in power of this strategy is also limited to 60 % of P_{PVmpp}.

$$P_{PV\_pred} = P_{Load\_pred} + P_{Bat\_ch\_pred} + P_{Feed\_in\_pred} \tag{III.6}$$

The operation principle of the strategy is depicted in figure 10. The control algorithms of mode A and D are similar to the previous strategies. In mode B and C however, $P_{Feed\text{-}in}$ and P_{Bat_ch} are optimized using the forecast data. If there is a difference between the measured and forecast data the feed-in power is corrected according Weniger et al. [6].Once the predicted time is reached, the battery is charged based on the value from the previous optimization [6], [14], [16].

During the charging period, the SOC of the battery is measured. The measured value is continuously compared to the predicted SOC in order to reduce the losses due to prediction errors. The correction is used as an input of an SOC controller and the output feeds a power controller. The power controller corrects the charging power to a new value $P_{Bat\_ch\_new}$ according to equation (III.7). This is done in order to achieve fully charged battery at the end of the day. If the measured SOC $SOC_{Bat_meas}$is less than the predicted SOC SOC_{Bat_pred}, the optimized power to charge the battery $P_{Bat\_ch\_new}$ is decreased and vice versa (see also figure 9):

$$P_{Bat\_ch\_new} = \frac{SOC_{Bat\_meas}}{SOC_{Bat\_pred}} \cdot P_{Bat\_ch\_pred} \tag{III.7}$$

In this simulation, perfect forecasts are used, and therefore, there is no deviation and correction of the predicted values. The strategy also uses reactive power compensation based on Q(U) control.

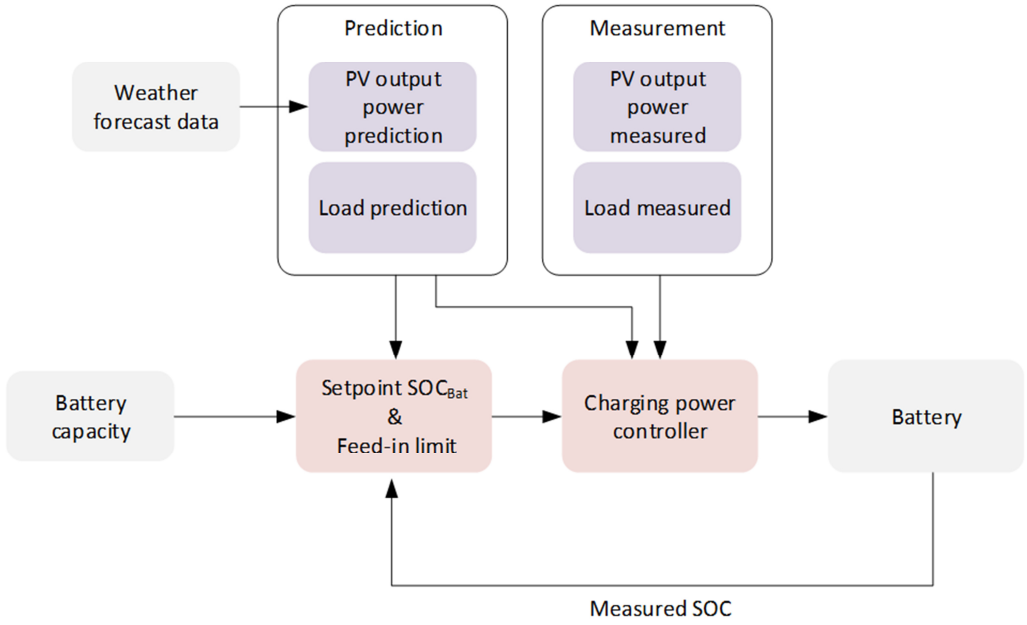

Figure 9: Schematic diagram of dynamic feed-in strategy

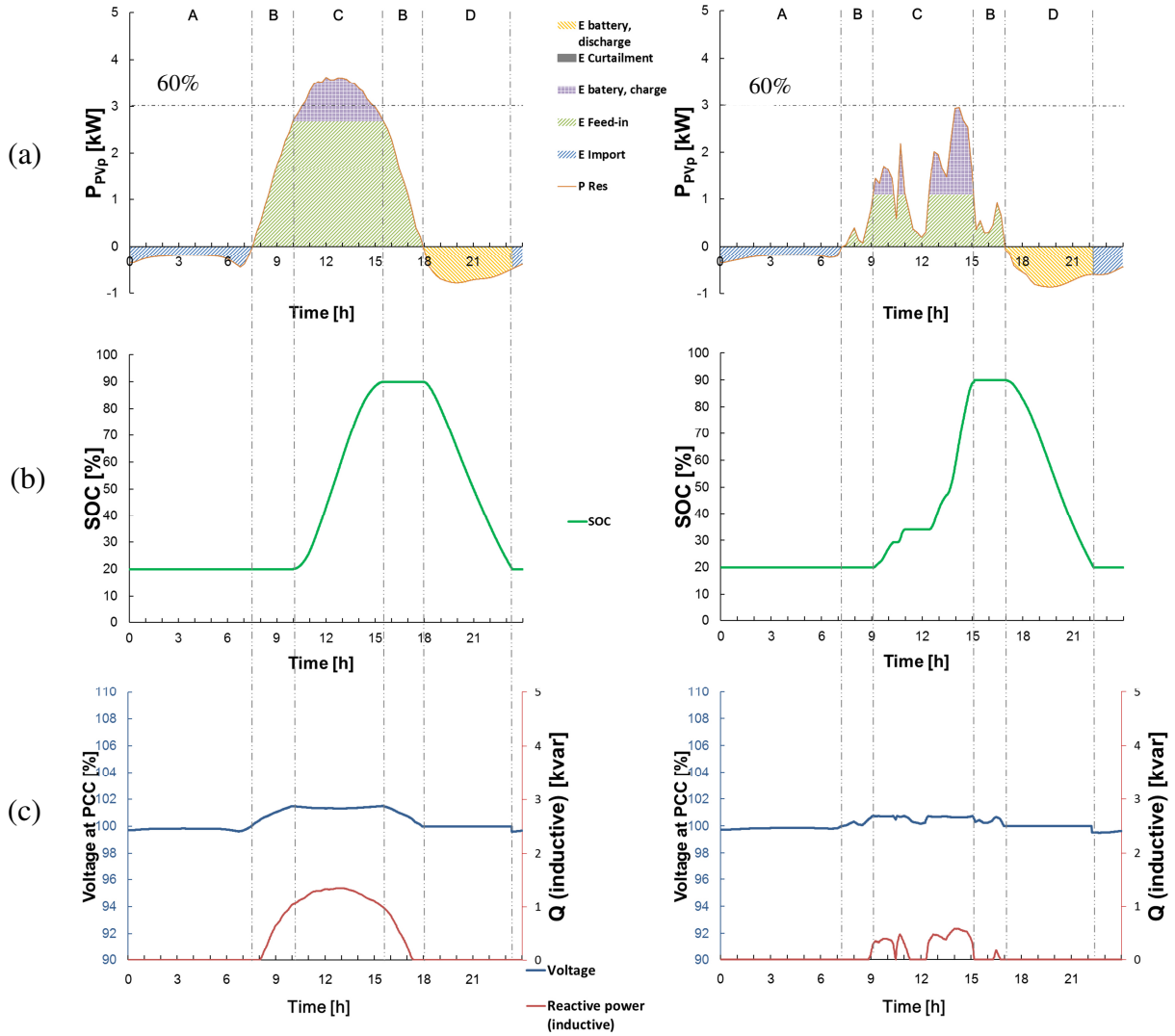

Figure 10: (a) power flows, (b) SOC and (c) voltage and reactive power at the PCC 12 of the dynamic feed-in strategy on a high (left) and a low (right) irradiance day

6. Dynamic feed-in limit with balancing

A dynamic feed-in limit with balancing capability strategy is proposed by Weniger et al. [6]. Principally, the algorithm is similar to the previous dynamic feed-in limit strategy. The difference is that the feed-in limit is set to a parabolic curve in order to compensate the feed-in peak of PV systems without a battery (mode C figure11). Therefore, the charging power is set to be high at midday. The advantage is that the PV storage systems using this strategy have the ability to balance the voltage in the feeder, if there are other PV systems that inject power into the grid around noon connected to the same feeder and therefore increase the voltage.

The strategy is promising for peak shaving and for balancing the grid. However, the power curtailment on the high irradiance day seems to be higher than the normal dynamic feed-in limit strategy (see figure 11).

Despite the ability to optimize the feed-in power limit and to reduce the voltage during peak feed-in, the main drawback of the general dynamic feed-in limit is the sensitivity of this strategy to the prediction errors. Overestimation of the prediction may lead to power curtailment and underestimation will reduce the self-consumption rate. High quality of weather forecast data from reliable forecasting technique is therefore required.

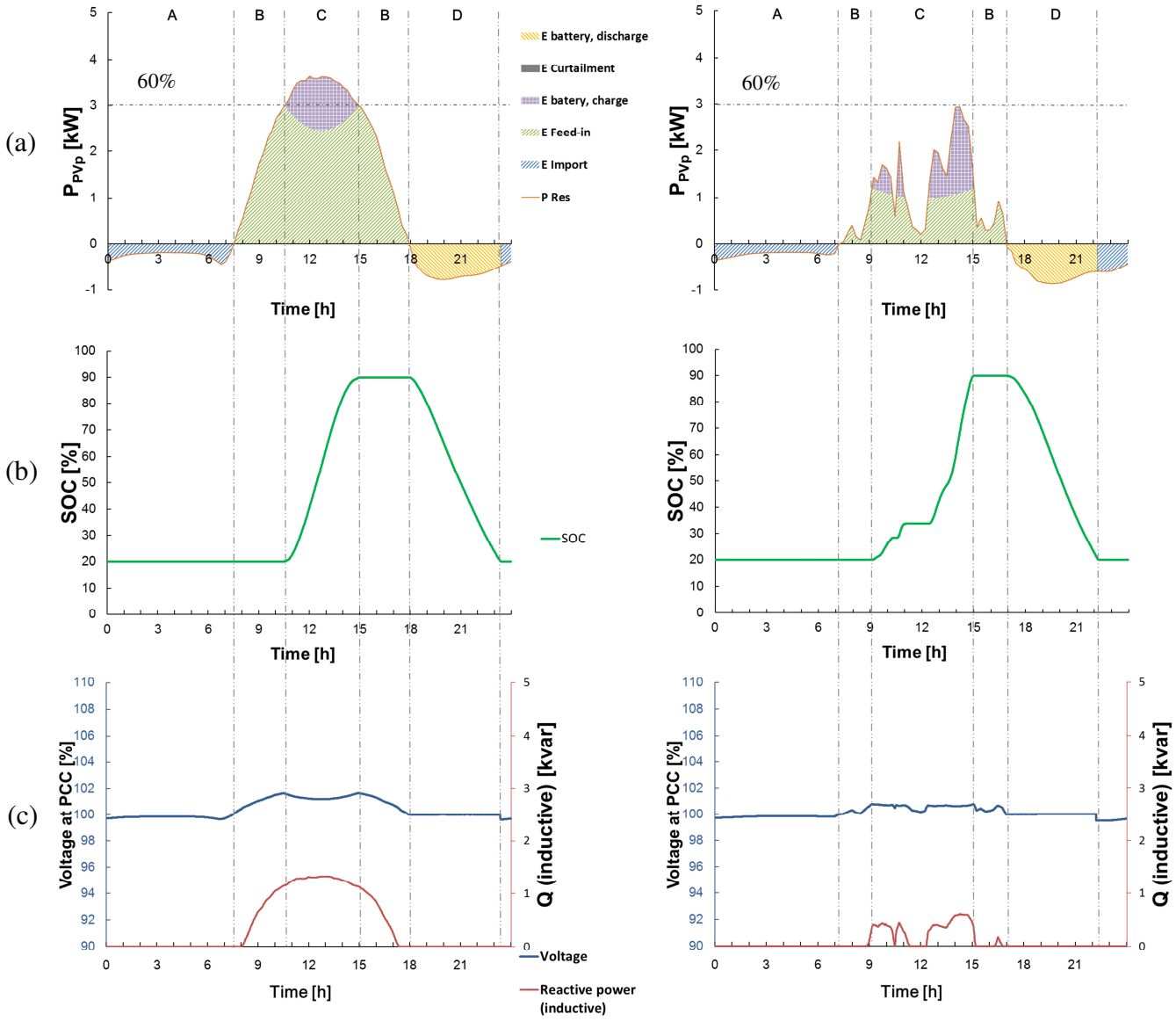

Figure 11: (a) power flows, (b) SOC and (c) voltage and reactive power at the PCC 12 of the dynamic feed-in with balancing strategy on a high (left) and a low (right) irradiance day

As forecast data are a must for the 5th and 6th control strategy. The following paragraph gives a short summery of the commonly used forecasting techniques.
Lödl et al. [17] uses a model based on the Spherical Harmonic Discrete Ordinate Method (SHDOM). The model uses global weather data to generate the global solar irradiation at ground level of the next days. The global weather data is interpolated to a detailed resolution to get the expected PV power on any position of PV power plants. An error analysis of the model has shown that the average error (rRMSE) of the weather forecast for the next day is 32.5%. The value increases for a longer forecast horizon. Another approach is to use persistence weather forecast. The forecasting method is based on extrapolating the current or recent PV power plant output taking into account the changing of the sun angle. Since the persistence is based on stochastic learning technique from historical pattern, the accuracy highly depends on the forecast horizon due to the change of cloudiness [18]. The forecast method is suitable for minute based forecasts for one location.

A similar PV forecast technique with learning algorithm is used by Williams et al. [16]. The method is to introduce a 30 % noise sequence to the hourly average of the true irradiance. The result of the prediction is 24 hours with hourly average and 30 % noises. It is claimed that the error is approximately the same as current numerical weather forecast in Central Europe.

The load prediction might also be derived using the persistence technique. Zeh et al. [15] proposes the load forecasting based on the load profile of past five days. The method is to divide the day into three periods: midnight to sunrise, sunrise to sunset and sunset to midnight. Using the arithmetic means of the past five days, the load profiles of each period defines the load for the next two days.
For simulation purposes, an autonomy forecasting using a learning algorithm is more preferable compare to the one that depends on the global weather data.

7. Feed-in damping

The feed-in damping strategy is almost identical to schedule mode with constant charging power (3rd strategy). The difference is that the feed-in damping uses a rough prediction of irradiance in order to define the charging time [15]. Figure 12 depicts the operation of the feed-in damping strategy. The control algorithms of mode A and D are similar to the previous strategies. In mode B however, the power to charge the battery is defined by dividing the spare charge in the battery with the predicted daytime with radiation. In order to avoid the losses due to forecast error, the charging power is varied by measuring the SOC of the battery in every simulation step. The battery is charged with constant power in the beginning, once residual power is higher than 60 % of P_{PVmpp}, the charging power is changed to the difference between residual power and feed-in power, as it is shown in mode C (figure 12 left). As soon as the residual power is below 60 % of P_{PVmpp}, mode B is reactivated and the power to charge the battery is recalculated.

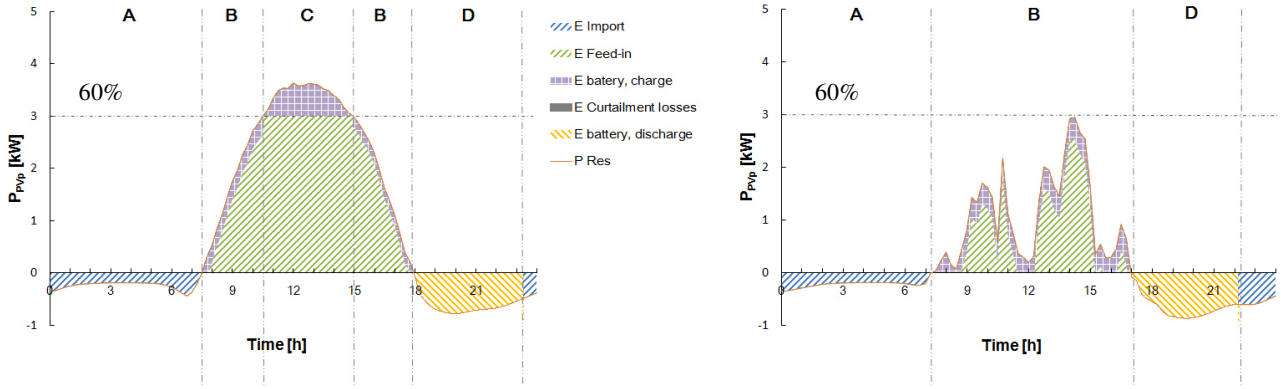

Figure 12: Power flows of the fixed feed-in strategy according to [10] on a high (left) and a low (right) irradiance day

The drawback of this strategy is the battery might not be fully charged at the end of the day. Since the prediction is only based on the predicted duration of residual power, there might be a possibility that at the end of the predicted time, the actual PV power is not the same as the calculated power.

IV. DISCUSSION

Seven control strategies have been investigated. Two scenarios on high and low irradiance day have been used to assess the strategies. Figure 13 displays the comparison of the strategies based on self-consumption ratio (SCR), self-supply ratio (SSR), and curtailment losses.

The self-consumption ratio and the self-supply ratio increase drastically by integrating a battery in the PV systems. For the scenario on a high irradiance day, all the strategies are able to fully charge the battery by the end of the day. The discrepancy appears during low irradiance days. The self-consumption ratio and the self-supply ratio of the strategy applying a schedule mode with constant charging power are slightly reduced due to insufficient irradiance during the defined schedule. The same happens with the feed-in damping strategy. Since the power to charge the battery and charging period is based on a rough prediction, the deviation between expected power and actual power at the end of the day causes a reduction of the self-consumption ratio.

A similar problem rises for the fixed feed-in strategy. The battery is charged only with the small surplus on the low irradiance day. Although a fixed feed-in power is equipped with the chance of charging the battery at the end of the day, the duration and the residual power is still not sufficient to significantly increase the SOC of the battery. Furthermore, with this strategy, there might be a possibility that the battery is not being charged if the residual power never reaches 50 % of P_{PVmpp}.

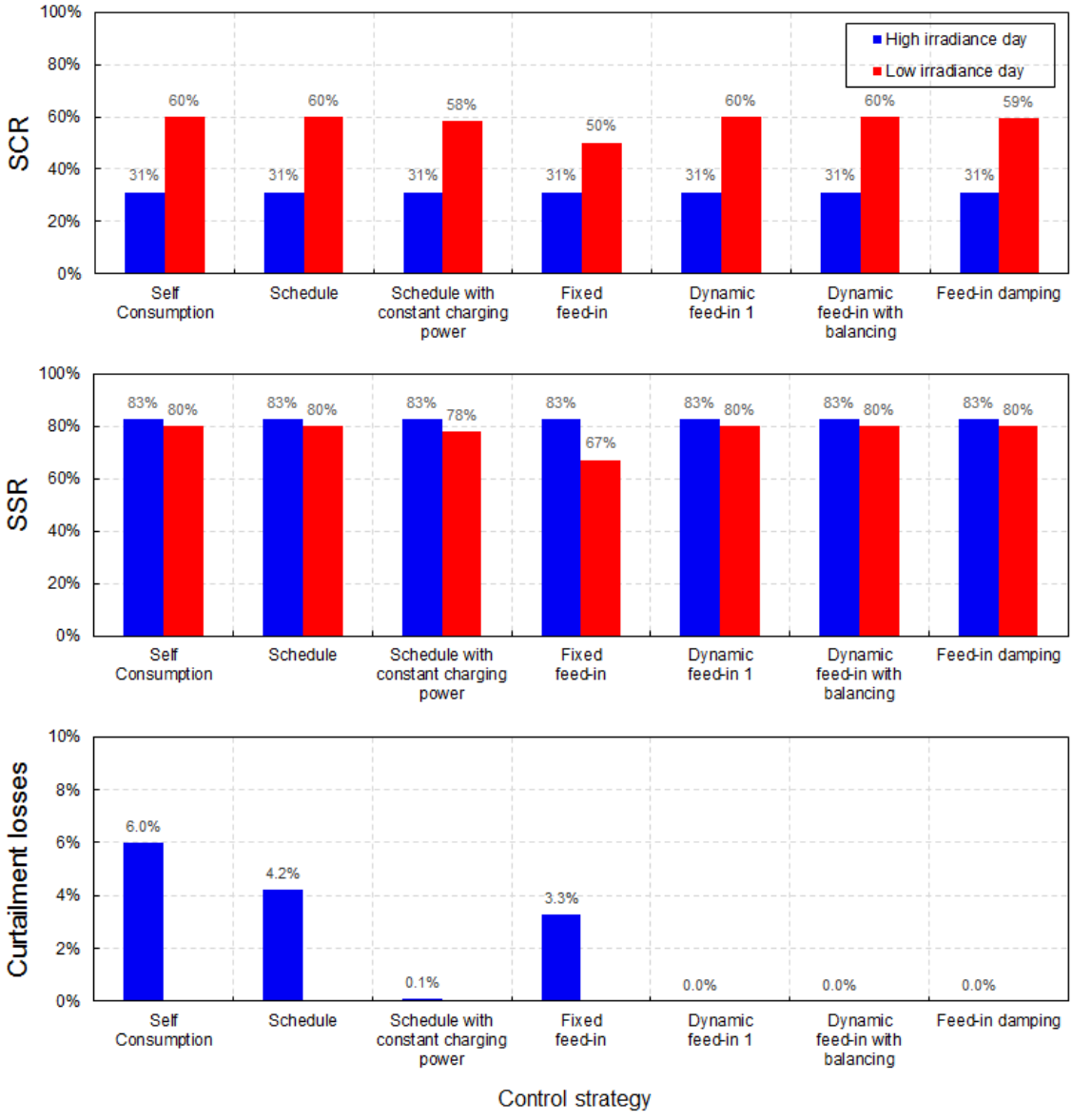

Figure 13: Comparison of the strategies based on the self-consumption ratio (SCR), the self-supply ratio (SSR), and curtailment losses

For the curtailment losses, the control strategies that use prediction data are able to reduce the curtailment losses to zero. This happens due to the perfect foresight assumption. The curtailment losses might increase if the forecast errors were considered. Besides, the schedule mode with constant charging shows low curtailment losses, too. That makes this strategy interesting, if no forecast data is available.

The ability to reduce the peak voltage can also be observed for all strategies (see figure 14). The observation is mainly focused on the day with high irradiance, because this may be considered the worst case. By limiting the feed-in power to 60 % a significant impact on the reduction of peak voltage is given. The voltage peak is suppressed even further by introducing a voltage support with reactive power compensation. The combination of these two methods leads to a voltage reduction with the minimum of 35 %. The state-of-the-art self-consumption strategy with power dependent reactive power control can reduce the voltage by 35 % (see pink curve) compared to a PV system that injects all its power into the grid (red curve "without control"). The reactive power control based on Q(U) increases the voltage reduction by an additional 7 % (not shown in figure 14).

The fixed feed-in limit strategy appears to be the best strategy to mitigate the voltage rise. A peak voltage reduction of 50 % is achievable by reducing the feed-in limit to 50 % (black curve). Furthermore, unlike most of the strategies that reach 60 % of feed-in limit during peak day, a dynamic feed-in limit strategy is able to reduce the feed-in power to about 56 %. Therefore the voltage is reduced by 48 % and this strategy might be considered as second best to reduce the voltage (orange curve).

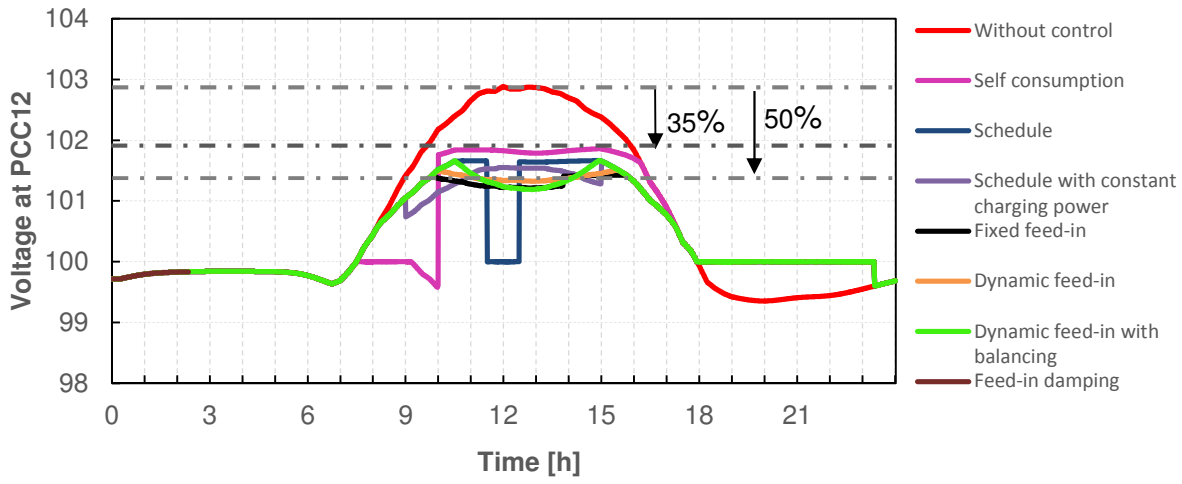

Figure 14: Comparison of voltage reduction at PCC12 on high irradiance day

From examining the operation of the control strategies, it can be deduced that the battery size influences the performance indicators. Increasing the battery size increases the self-consumption rate and the self-supply rate in some extent. The curtailment losses of each strategy are reduced by an increasing battery size, especially for the strategy that uses the surplus between the residual and the feed-in power to charge the battery. From a voltage reduction perspective, the impact of the bigger battery can be optimized by implementing a schedule mode with a constant charging power, fixed feed-in, dynamic feed-in, and feed-in damping strategies.

Each of the simulated strategies has its advantages and disadvantages. The schedule modes show only the advantage of reducing the curtailment losses. The schedule with constant charging power has low curtailment losses on the day with high irradiance, but the problem is raised when there is not sufficient irradiance during the charging period.

Although the fixed feed-in is the best in reducing peak voltage, the strategy shows low self-consumption and self-supply ratios during the low irradiance day and a considerable curtailment losses during high irradiance day of 3.3 %. These limitations make this approach less favorable to improve the benefit of having a PV storage system.

The dynamic feed-in strategy is more favorable due to its ability to get a high self-consumption rate, self-supply rate, low curtailment losses, and high peak voltage reduction. This is achieved by adjusting the feed-in power based on the weather and load predictions. Although no forecast errors

have been taken into account, it is expected that the error´s impact is considerably small due to the possible self-correction of the feed-in power limit within the charge controller (see figure 9). Furthermore, Schneider et al. [14], Struth et al. [9] and William et al. [16] also report that the dynamic feed-in is preferable to self-consumption, schedule mode, and schedule mode with constant charging power strategies. Dynamic feed in with balancing might be useful for the grid with a mix of PV systems without a battery and PV storage systems that are equipped with this strategy.

Furthermore, the feed-in damping strategy has also shown promising results. The main advantage of feed-in damping over dynamic feed-in is that the strategy does not need a high quality of prediction data. As a consequence, the performance of the strategy is weaker than dynamic feed-in. However, Zeh et al. [15] concludes that the feed-in damping is more recommended than dynamic feed-in as it is less sensitive to forecast errors and has a higher self-consumption ratio. This contradictory conclusion cannot be observed in this study due to the limitation on two sample days and the assumption of no forecasts error.

V. CONCLUSION

The comparison of different control strategies based on self-consumption rate, self-supply rate, curtailment losses, and peak voltage reduction (PVR) has been presented. A qualitative comparison of all control strategies is concluded in table 2.

Tab. 2 Results of the qualitative comparison of the analysed control strategies

Control strategy	SCR	SSR	CLR	PVR
Self-consumption	+++	+++	+	+
Schedule	+++	+++	+	++
Schedule with constant charging power	++	++	++	++
Fixed feed-in	+	+	+	+++
Dynamic feed-in	+++	+++	+++	+++
Dynamic feed-in with balancing	+++	+++	+++	++
Feed-in damping	+++	+++	+++	++

It can be concluded, that the utilization of storages may increase the self-consumption ratio and the self-supply ratio for all seven control strategies. The simulation results have shown that implementing a smarter control strategy will give a significant improvement of the CLR and PVR compared to the common straight forward self-consumption strategy.

The analysis of the dynamic feed-in strategy has shown that PV storage systems might have a high self-consumption ratio while still being able to reduce the peak voltage. Based on the results on the two scenarios, it can be concluded that the dynamic feed-in limit is the most favorable strategy to be implemented (see dark blue row, table 2). The second option is the feed-in damping strategy. As it is claimed in previously, this strategy has a low self-consumption rate and is less sensitive to the prediction errors (see light blue row, table 2). Lastly, the schedule mode with constant charging power could be considered for the strategy without forecast data.

In future studies the effects of the control strategies on the grid and the benefit for the PV storage system owner could be simulated in detail. The aim would be to implement the self-consumption, the dynamic feed-in limit, and feed-in damping strategy in PSS Sincal. The assessment would be done with a simulation of an entire year to see a clear distinction between the strategies. Instead of using a reference grid, the simulation could be done by using the real grid with a high share of residential PV systems. In order to get a broader view of the share of losses, the efficiency of the inverter and battery could be taken into account. Another step to quantify the results better would be to use the weather and load forecasts models and implement them to the control strategies by using an autonomy forecast based on a learning algorithm.

Acknowledgements

The research was funded by the Federal Ministry of Economics and Technology (BMWi) under grant agreement no. 0325522A. We thank also the joint research partners Brisa Ortiz from the SMA AG, Sebastian Aschenbrenner and Dr. Peter Schwägerl from the Lechwerke Verteilnetze GmbH (LVN) as well as Marcel Galle and Dr. Bernd Kalks of the Younicos AG for their great support during different steps of this project. Furthermore, we thank Dr. Ilja Pawel from the Cellstrom GmbH, which is a subsidiary of DMG Mori Seiki AG, for the support on the battery side.

References

[1] Marra, F., Yang, G., Træholt, C., Østergaard, J., Member, S., and Larsen, E. "*A decentralized storage strategy for residential feeders with photovoltaics"*, IEEE transactions on smart grid, (2013).

[2] DIN Deutsches Institut für Normung e. V., "*Merkmale der Spannung in öffentlichen Elektrizitätsversorgungsnetzen; Deutsche Fassung EN 50160:2010 + Cor. :2010",* (2011).

[3] J. Cappelle, J. Vanalme, S. Vispoel, T. Van Maerhem, B. Verhelst, C. Debruyne, and J. Desmet, "*Introducing small storage capacity at residential PV installations to prevent overvoltages"*, *2011 IEEE Int. conference smart grid communications.*, pp. 534–539, (2011).

[4] VDE Verband der Elektrotechnik Elektronik Informationstechnik e. V., "*VDE-AR-N 4105 Erzeugungsanlagen am Niederspannungsnetz – Technische Mindestanforderungen für Anschluss und Parallelbetrieb von Erzeugungsanlagen am Niederspannungsnetz"*, p. 80, (2011).

[5] M.Wimmer, O.Weber, K. Freier, "*The market incentive programme for battery storage systems – first experiances"*, 8th International Renewable Energy Storage Conference and Exhibition (IRES), (2013).

[6] J. Weniger, T. Tjaden, and V. Quaschning, "*Sizing and grid integration of residential PV battery systems",* 8th International Renewable Energy Storage Conference and Exhibition (IRES), (2013).

[7] C. Fünfgeld and R. Tiedemann, "*Anwendung der Repräsentativen VDEW-Lastprofile step by step"*, VDEW Materialien, vol. M–05/2000, (2000).

[8] G. Kerber, "*Aufnahmefähigkeit von Niederspannungsverteilnetzen für die Einspeisung aus Photovoltaikkleinanlagen"*, PhD thesis, TU München, (2011).

[9] J. Struth, K. Kairies, M. Leuthold, A. Aretz, P. B. Hirschl, P. A. Schnettler, P. Dirk, U. Sauer, M. Bost, S. Gährs, M. Cramer, and E. Szczechowicz, "*PV-BENEFIT : A CRITICAL REVIEW OF THE EFFECT OF GRID INTEGRATED PV-STORAGE-SYSTEMS"*, 8th International Renewable Energy Storage Conference and Exhibition (IRES), (2013).

[10] J. von Appen, T. Stetz, M. Braun, and A. Schmiegel, "*Local Voltage Control Strategies for PV Storage Systems in Distribution Grids,*" IEEE Trans. Smart Grid, vol. 5, no. 2, pp. 1002–1009, (2014).

[11] E. Man, "*Control of grid connected PV systems with grid support functions*," Tech. rep., Aalborg University, (2012).

[12] Y. Ueda, K. Kurokawa, K. Kitamura, K. Akanuma, M. Yokota, and H. Sugihara, "*Study on the overvoltage problem and battery operation for grid-connected residential PV systems*," 22nd Eur. Photovolt. Sol. Energy Conf., pp. 3094–3097, (2007).

[13] Westnetz GmbH, "*Technische Anschlussbedingungen Niederspannung*," (2013).

[14] M. Schneider, P. Boras, H. Schaede, L. Quurck, and S. Rinderknecht, "*Effects of Operational Strategies on Performance and Costs of Electric Energy Storage Systems*," Energy Procedia,

vol. 46, no. Ires 2013, pp. 271–280, (2014).

[15] A. Zeh and R. Witzmann, "*Operational strategies for battery storage systems in low-voltage distribution grids to limit the feed-in power of roof-mounted solar power systems*," Energy Procedia, vol. 46, pp. 114–123, (2014).

[16] C. Williams, J. Binder, M. Danzer, F. Sehnke, and M. Felder, "*Battery charge control schemes for increased grid compatibility of decentralized PV systems*," 28th Eur. Photovolt. Sol. Energy Conf. Exhib., (2013).

[17] M. Lödl, R. Witzmann, and M. Metzger, "*Operation strategies of energy storages with forecast methods in low-voltage grids with a high degree of decentralized generation*," 2011 IEEE Electrical Power and Energy Conference, pp. 52–56, (2011).

[18] S. Pelland, J. Remund, J. Kleissl, T. Oozeki, and K. De Brabandere, "*Photovoltaic and solar forecasting: state of the art*," IEA PVPS Task 14 Subtask 3.1 Tech. Rep., International energy agency (IEA), (2013).